Solid-state high-resolution NMR studies on spin density distribution of a ferromagnetic coordination polymer: $Ni(NCS)_2(Him)_2$

Goro Maruta * Sadamu Takeda

Division of chemistry, Graduate School of Science, Hokkaido University, Sapporo, 060-0810, Japan

Abstract

We determined hyperfine coupling constants (hfcc) of the imidazole ligand in a ferromagnetic coordination polymer, di-μ-thiocyanatobis(imidazole)nickel(II), using ^{1}H-, ^{2}H-, and ^{13}C-MAS-NMR. Partially or fully deuterated sample was prepared to measure temperature dependence of the isotropic shifts of NMR signals. We obtained hfcc of $A_{\mathrm{C}} = +0.57$, $+0.69$, $+1.88$ MHz for 2-, 4-, 5-carbon and $A_{\mathrm{H}} = +0.66$, $+0.37$, $+0.48$, $+0.53$ MHz for 1-, 2-, 4-, 5-proton in the imidazole ligand, respectively, which indicates that unpaired electron in $d_{x^2-y^2}$ orbital of Ni(II) ion delocalizes over the imidazole ligand. On the basis of the NMR and DFT results, we proposed an interchain superexchange pathway through N–H $\cdots$ S hydrogen bond.

Key words: imidazole, solid-state high-resolution NMR, magnetic property, coordination polymer, spin density distribution

* Corresponding author. Tel.: +81 11-706-3504; Fax:+81 11-706-4841.
Email address: maruta@sci.hokudai.ac.jp (Goro Maruta).

1 Introduction

Magnetic interactions in coordination compounds can be classified into three groups: direct, intramolecular, intermolecular interactions. The direct interaction is the interaction between paramagnetic metal ions connected by direct metal-metal bond. The other two interactions are mediated by diamagnetic ligands and are indispensable for a molecule-based magnet to exhibit long range order such as ferromagnetism, ferrimagnetism, and antiferromagnetism.[1,2] The intramolecular magnetic interaction is the interaction mediated by bridging ligands in a polynuclear complex. Not only simple ligands (Cl^-, Br^-, O^{2-}, OH^-) but also bidentate ligands (SCN^-[3], ox^-[4], N_3^-[5]) can act as a magnetic coupler. The role of these bridging ligands in the superexchange interaction can be explained well by a molecular orbital theory at the level of extended Hückel calculation. And the theory can be verified from spin density distribution determined by polarized neutron diffraction experiment.[6]

In contrast, The intermolecular magnetic interaction, which contains van der Waals contact or hydrogen bonding in its interaction pathway, has not been understood well because this interaction is relatively weak and it may depend on crystal packing. This interaction plays an important role when pseudo low-dimensional magnetic compound undergoes three-dimensional ordered state. An example is diimidazolecopper(II) dichloride [7,8]. In this crystal, one-dimensional Cu(II) chain is formed by bridging Cl ion, and the magnetic susceptibility data above 12 K is interpreted by one-dimensional antiferromagnetic Heisenberg model with $J = -2.1$ cm^{-1}. However, it undergoes three-dimensional antiferromagnetic ordering below 7.7 K, indicating interchain antiferromagnetic interaction. This interchain interaction is probably

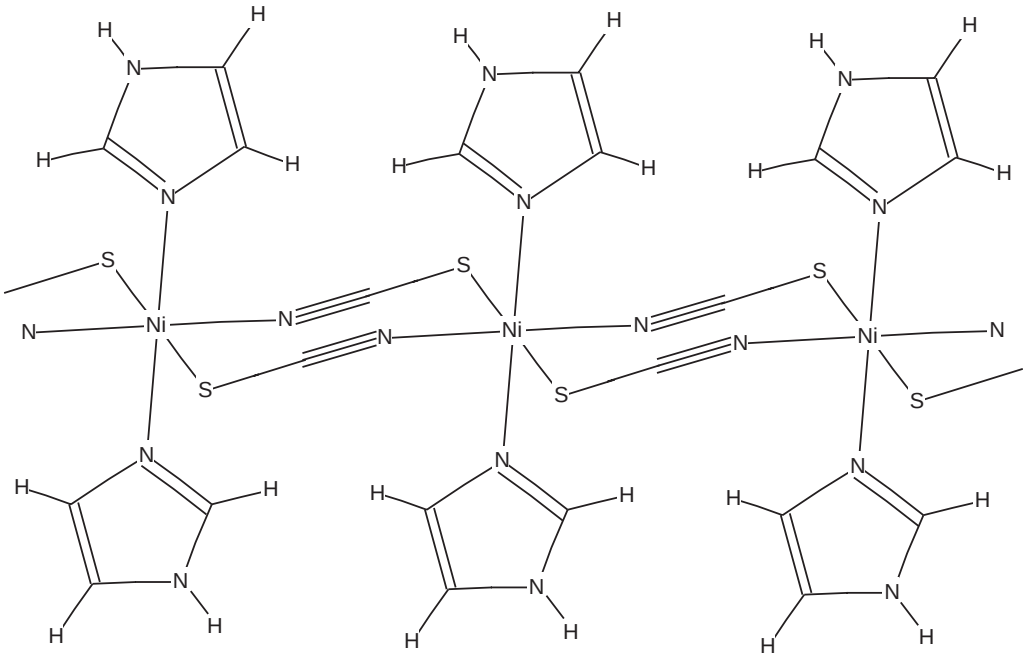

Fig. 1. One dimensional chain structure of $Ni(NCS)_2(Him)_2$.

mediated by N–H $\cdots$ Cl hydrogen bond between adjacent chains but its coupling mechanism is still unknown. Moreover, imidazole ligand seems to act as ferromagnetic coupler in another compound.[3] Higher level of theory and experimental methods to verify this theory are necessary to understand the intermolecular magnetic interaction in coordination compounds. In this work, we have employed Density functional theory (DFT) and NMR experiment[9] to elucidate role of the imidazole ligand in long range ordering.

Di-μ-thiocyanatobis(imidazole)nickel(II), $Ni(NCS)_2(Him)_2$, is a ferromagnet (T_C = 5 K) which consists of NCS-bridged one-dimensional Ni(II) chains as shown in Fig. 1 with the intrachain exchange interaction parameter ($2J$) of 8.0 cm^{-1}.[3] In this work, we determined electron spin density distribution of imidazole ligand in the compound by measuring solid-state high-resolution ^{1}H-, ^{2}H-, and ^{13}C-NMR spectra in order to elucidate the interchain magnetic interaction essential for long-range order in the crystal. Partially or fully

deuterated imidazole was used to prepare the sample and magic angle spinning (MAS) technique was employed to measure temperature dependence of the isotropic shifts of NMR signals. These experimental results indicate that unpaired electrons in the d-orbitals of the octahedral nickel(II) ion delocalize over the imidazole ligand. Consequently, we proposed an interchain superexchange pathway through N–H $\cdots$ S hydrogen bond.

2 Experimental

2.1 Preparations

1,2-Dideutero-imidazole was prepared by literature method [10]. The degree of deuteration was estimated to be 70-80 %. $Ni(NO_3)_2 \cdot 6D_2O$ was recrystallized from deuterium oxide. 1,2,4,5-Tetradeutero-imidazole (98 % D, Cambridge Isotope Laboratories) and the other reagents were used as supplied. Non-deuterated sample of $Ni(NCS)_2(Him)_2$ (**1**) was prepared by a similar method described in Ref [3]. $Ni(NO_3)_2 \cdot 6H_2O$ (2 mmol) and NaSCN (4 mmol) were dissolved in water (2 cm^3), then the aqueous solution was added to methanol solution (1 cm^3) of imidazole (4 mmol). The resulting blue solution was left to stand under N_2 gas flow at room temperature. Green crystal of $Ni(NCS)_2(Him)_2$ was obtained with violet crystal of $Ni(NCS)_2(Him)_4$. The products were separated by hand, washed with water and acetone, and dried in vacuo. Fully deuterated sample of $Ni(NCS)_2$(1,2,4,5-tetradeutero-Him)$_2$ (**4**) was prepared from 1,2,4,5-tetradeutero-imidazole with deuterated solvents of D_2O and CH_3OD. Partially deuterated samples of $Ni(NCS)_2$(1,2-dideutero-Him)$_2$ (**3**) and $Ni(NCS)_2$(2-deutero-Him)$_2$ (**2**) were prepared from

1,2-dideutero-imidazole with deuterated and protonated solvents, respectively.

2.2 NMR measurements

Solid-state high-resolution ^{1}H-, ^{2}H-, and ^{13}C-NMR spectra of $\mathbf{1}-\mathbf{4}$ were measured at a resonance frequencies of 300, 46.1, and 75.4 MHz, respectively, with a Bruker DSX300 spectrometer and a 4-mm CP/MAS probe. Temperature dependence of the spectra were measured for **3** from 300 K to 200K. Magic angle spinning (MAS) technique was used to obtain high-resolution spectra for the powder samples, whereas cross polarization or ^{1}H-decoupling was not employed. The spinning rates of the samples were 9-10 kHz. The free induction decay (FID) of ^{1}H-MAS-NMR was accumulated from the first rotational echo after a $\pi/2$ pulse. For ^{2}H- or ^{13}C-MAS-NMR, π pulse was applied at the first rotational echo after a $\pi/2$ pulse,then the FID was accumulated from the second rotational echo. The repetition time for each spectrum was 0.5 s. The thermometer of the MAS probe was calibrated against the isotropic chemical shift of the ^{207}Pb-MAS-NMR spectrum of $Pb(NO_3)_2$ [11]. The uncertainty of the temperature measurement after the calibration was 4 K, and the temperature fluctuation during the accumulation was within 1 K. The differences between the sample temperature T and the bearing gas temperature T_b, which was read from the thermometer, were 27 K at $T = 202$ K and 7 K at $T = 304$ K for a spinning rate of 9 kHz [12]. ^{1}H-, ^{2}H-, and ^{13}C-NMR shifts were measured from tetramethylsilane.

2.3 Computational methods

Using the GAUSSIAN 98 software package [13], we performed UB3LYP calculation on $[Ni(NCS)_2(SCN)_2(Him)_2]^{2-}$ as a molecular model for the coordination polymer. The geometric structure of the model was extracted from the crystal structure [3] determined by X-ray diffraction. The Wachters-Hay basis set [14,15] was used for Ni atom and the 6-31G(d,p) basis set was used for H, C, N, S atoms.

3 Results and discussion

3.1 NMR peak assignment

The observed isotropic lines in the ^{2}H-MAS-NMR spectra were accompanied by typically 30 spinning sidebands (SSBs) spaced at the spinning frequencies. This is because the anisotropic quadrupole interactions of the deuterons are much larger than the spinning frequencies. We confine ourselves to the isotropic part of the spectra though it is possible, in principle, to analyze the SSBs to deduce the anisotropic hyperfine interaction [16]. Figure 2(a) shows the central part of the ^{2}H-NMR spectrum of **3** measured at a spinning frequency of 9 kHz. Two isotropic lines corresponding to 1,2-deuterons of the imidazole ligand were observed at 69 ppm and 46 ppm. A signal at 6 ppm was assigned to a trace of solvent because it flanked no SSBs. In the ^{2}H-NMR spectrum of **2**, in which only 2-position of the imidazole ligand is deuterated, the peak at 69 ppm was disappeared. Thus we assigned this peak to 1-deuteron and the peak at 46 ppm to 2-deuteron of imidazole. Figure 2(b) shows the ^{1}H-NMR

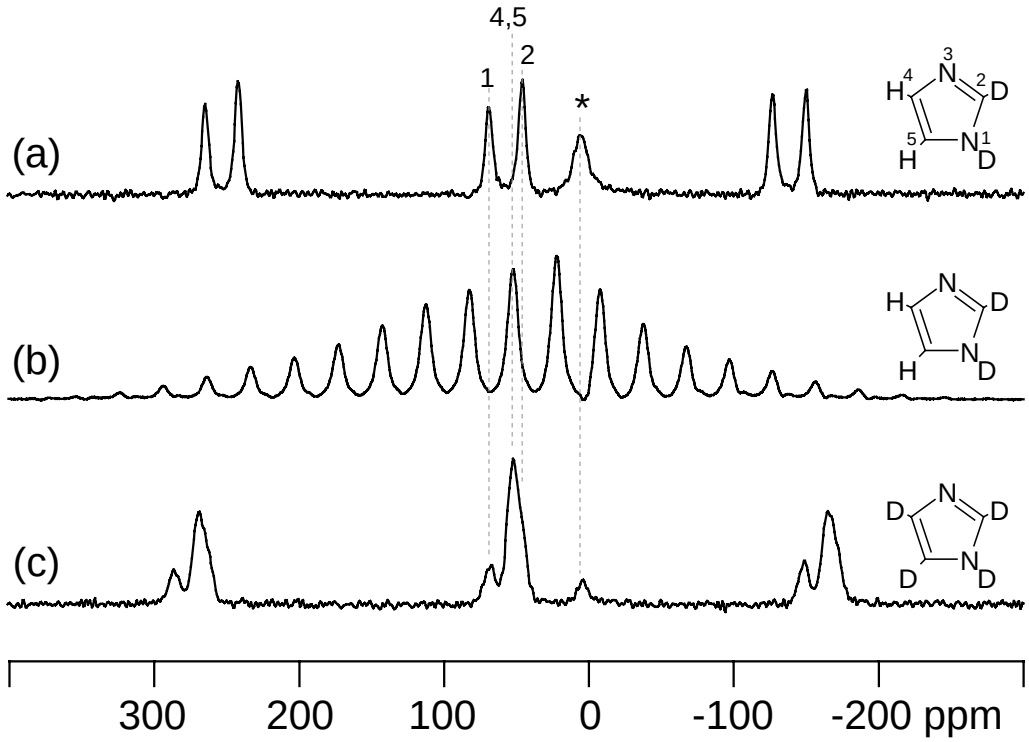

Fig. 2. (a)^{2}H-MAS-NMR spectrum of **3** at 9 kHz and 304 K. (b)^{1}H-MAS-NMR spectrum of **3** at 9 kHz and 304 K. (c)^{2}H-MAS-NMR spectrum of **4** at 10 kHz and 306 K. Asterisk indicates trace of solvent.

spectrum of **3** measured at a spinning frequency of 9 kHz. An isotropic line at 52 ppm was assigned to unresolved signals of 4,5-protons of the imidazole ligand. This overlap of the two peaks could not be removed in the ^{2}H-MAS-NMR spectrum of fully deuterated **4** at a spinning frequency of 10 kHz as shown Fig. 2(c). In this spectrum, the signal of 2-deuteron also overlapped those of 4,5-deuterons. We, therefore, measured temperature dependence of ^{2}H- and ^{1}H-MAS-NMR spectra of **3** to obtain the hyperfine coupling constants of the hydrogen atoms of the imidazole ligand.

Figure 3(a) shows ^{13}C-MAS-NMR spectrum of **1** at a spinning frequency of 10 kHz and 306 K. Three isotropic lines were observed at 564, 318, 278 ppm though four inequivalent carbon sites exist in the crystal. We considered that

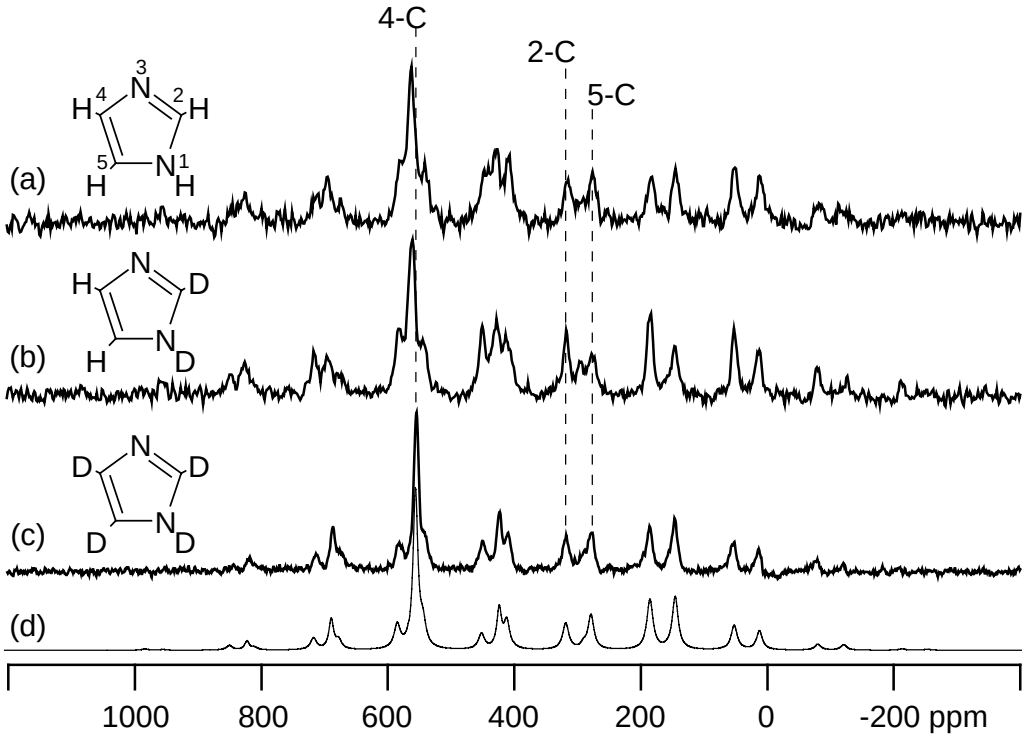

Fig. 3. ^{13}C-MAS-NMR spectra of (a) **1**, (b) **3**, (c) **4** at a spinning frequency of 10 kHz and 306 K. Three isotropic lines of 561, 318 and 277 ppm are assigned to 4-, 2-, and 5-carbon, respectively. (d) ^{13}C-MAS-NMR spectrum synthesized with the parameters Δ^{calc} and η^{calc}.

the signal of ^{13}C in the thiocyanate ligand broadened out to baseline because of its fast transverse relaxation rate T_2^{-1} caused by large hfcc of this nucleus. We, consequently, assigned all the observed three lines to ^{13}C in the imidazole ligand. The peak at 318 ppm and its SSBs sharpened when protons of 1,2-position were substituted by deuterons as shown in Fig. 3(b). This narrowing is explained by the facts that (i) ^{13}C-^{1}H dipolar interaction is not completely removed under our MAS condition, and (ii) the nuclear-nuclear dipolar interaction can be reduced chemically by deuteration. The degree of the reduction should be most significant for the adjacent carbon. Thus we assigned the peak at 318 ppm to 2-carbon. When all the protons were substituted by deuterons, all the lines in ^{13}C-NMR spectrum sharpened as shown in Fig. 3(c). We ana-

Table 1

Anisotropic and asymmetric parameters in 2,4,5-carbon of the imidazole ligand of $Ni(NCS)_2$(Him-d_4)$_2$ at 306 K.

position	δ_{iso}/ppm	Δ^{exp}/ppm	Δ^{calc}/ppm	η^{exp}	η^{calc}
2-carbon	318	520	530	0.8	0.4
4-carbon	555	240	207	0.8	0.6
5-carbon	278	440	450	0.7	0.6

lyzed the SSB pattern of this spectrum to assign the remaining two peaks. In general, we can extract the principal values $\delta_{xx}, \delta_{yy}, \delta_{zz}$ of the NMR shift tensor from SSB pattern of ^{13}C-MAS-NMR spectrum [17]. These parameters can be expressed by another set of parameters, $\delta_{iso} = (\delta_{xx}+\delta_{yy}+\delta_{zz})/3$, $\Delta = \delta_{zz}-\delta_{iso}$, $\eta = (\delta_{xx}-\delta_{yy})/\Delta$, where $|\delta_{zz}| \geq |\delta_{xx}| \geq |\delta_{yy}|$. Using WIN-FIT [18] program, we fitted the ^{13}C-MAS-NMR spectrum of **4** with CSA mas model. The optimized parameters, δ_{iso}, Δ^{exp}, η^{exp}, are listed in Table 1. We found that the position of the isotropic line δ_{iso} of the signal at the highest frequency shifted from 564 ppm (**1** and **3**) to 555 (**4**) ppm by deuteration. The other two peak (318 and 278 ppm) remained the same within experimental errors. The cause of this shift is not fully understood at present. we guess that it was due to a slight modification of the crystal structure caused by deuterium substitution. The anisotropic parameter Δ^{exp} of the highest frequency peak was smaller than those of the other peaks, indicating this signal can be assigned to 4-carbon of which distance from nickel atom is long. To confirm this speculation, we computed anisotropic parameter Δ^{calc} and the asymmetric parameter η^{calc} for each carbon site from crystal structure parameters as discussed below.

Supposing the nuclear-nuclear dipolar interaction is decoupled, the NMR shift

tensor is given as a sum of the hyperfine tensor and the chemical shift tensor [19]. The anisotropic part of the hyperfine tensor, which comes from electron-nuclear dipolar interaction, can be estimated by a point dipole model [20]. We put a point dipole bearing effective moment of $\mu_{\rm eff} = g\sqrt{S(S+1)} = 2.18\sqrt{2}$ on each octahedral NiS_2N_4 unit. The spin distribution was taken to be 76 % (nickel), 5 % (sulfur), 4 % (nitrogen of the thiocyanate), and 3 % (nitrogen of the imidazole) on the basis of the DFT calculation. NiS_2N_4 units within 30 Å of the carbon were taken into account to calculate the dipolar field at 2,4,5-positions of the imidazole. The chemical shift tensor of each carbon was estimated from UB3LYP calculation on the molecular model. The hyperfine and the chemical-shift tensors were added together and diagonalized to obtain $\Delta^{\rm calc}$ and $\eta^{\rm calc}$. The parameters computed for each carbon site are listed in Table 1. The computed anisotropic parameters $\Delta^{\rm calc}$ were consistent with $\Delta^{\rm exp}$, whereas agreement between asymmetric parameters $\eta^{\rm calc}$ and $\eta^{\rm exp}$ was not very good. This is probably due to low accuracy of the estimates of the chemical shift tensor. However, the agreement was sufficient for the purpose of assigning the two signals at 555 and 278 ppm to 4-carbon and 2-carbon, respectively. The ^{13}C-MAS-NMR spectrum of **4** is well reproduced by a spectrum synthesized with the parameters $\Delta^{\rm calc}$ and $\eta^{\rm calc}$ (Fig. 3(d)), supporting the peak assignment.

3.2 Determination of the hyperfine coupling constants

The hyperfine coupling constants (hfcc) of the ^{1}H, ^{2}H and ^{13}C of the imidazole ligand were determined from the temperature dependence of the isotropic NMR shifts $\delta_{\rm iso}$ measured for **3** using the following procedure.

The isotropic shift of a ligand nucleus in a paramagnetic metal complex consists of the Fermi contact term, the pseudo contact term, and the diamagnetic term

$$\delta_{\mathrm{iso}} = \delta_{\mathrm{Fermi}} + \delta_{\mathrm{pc}} + \delta_{\mathrm{dia}}. \tag{1}$$

Kurland and McGarvey [21] gave a expressions for δ_{Fermi} and δ_{pc} of tetragonally distorted octahedral Ni^{2+} ($S = 1$) complex as

$$\delta_{\mathrm{Fermi}} = \frac{2g_{\mathrm{iso}}\mu_{\mathrm{B}}A}{3k_{\mathrm{B}}T(\gamma_{\mathrm{nuc}}/2\pi)}\left[1 - \frac{g_{\parallel} - g_{\perp}}{9g_{\mathrm{iso}}}\frac{D}{k_{\mathrm{B}}T}\right] \tag{2}$$

$$\delta_{\mathrm{pc}} = \frac{2\mu_{\mathrm{B}}^2(g_{\parallel}^2 - g_{\perp}^2)}{9k_{\mathrm{B}}T}\frac{3\cos^2\Omega - 1}{R^3}\left[1 - \frac{g_{\parallel}^2 - g_{\perp}^2/2}{3(g_{\parallel}^2 - g_{\perp}^2)}\frac{D}{k_{\mathrm{B}}T}\right], \tag{3}$$

where A is the hfcc in hertz, T is the absolute temperature, γ_{nuc} is the gyromagnetic ratio of the nucleus, $g_{\parallel}$ and $g_{\perp}$ are the parallel and perpendicular components of the g tensor, D is the zero field splitting parameter, R is the length of a vector from the metal to the nucleus, Ω is the angle between the vector and z-axis, and the other terms have their usual meanings. The zero field splitting of $Ni(NCS)_2(Him)_2$ is so small ($D/k_{\mathrm{B}}T < 2 \times 10^{-3}$ for $T > 200$ K) that we dropped the second terms of these equations. The intrachain magnetic interaction of the coordination polymer was included by substituting $T \to T - \theta$ where θ is the Weiss temperature. Then we obtained

$$\delta_{\mathrm{Fermi}} = \frac{2g_{\mathrm{iso}}\mu_{\mathrm{B}}A}{3k_{\mathrm{B}}(T - \theta)(\gamma/2\pi)} \tag{4}$$

$$\delta_{\mathrm{pc}} = \frac{2\mu_{\mathrm{B}}^2(g_{\parallel}^2 - g_{\perp}^2)}{9k_{\mathrm{B}}(T - \theta)}\frac{3\cos^2\Omega - 1}{R^3}. \tag{5}$$

To determine A from the temperature dependence of δ_{iso}, we estimated the other parameters $g_{\parallel}$, $g_{\perp}$, and θ from published data. The Weiss temperature were estimated from the intrachain magnetic coupling constant $2J = 8.0$ cm^{-1}

[3], using

$$\theta = \frac{2zS(S+1)}{3k_{\mathrm{B}}}J \tag{6}$$

where z is the number of the neighboring atoms and is equal to two for a simple magnetic chain. The estimated value of θ is 15.3 K. The g values of tetragonally distorted octahedral Ni^{2+} ($S = 1$) complex can be expressed as

$$g_{\perp} = 2.0023 - \frac{8\lambda}{\Delta E(^3\mathrm{B}_{1\mathrm{g}} \rightarrow {}^3\mathrm{E}_{\mathrm{g}})} \tag{7}$$

$$g_{\parallel} = 2.0023 - 8\frac{8\lambda}{\Delta E(^3\mathrm{B}_{1\mathrm{g}} \rightarrow {}^3\mathrm{B}_{2\mathrm{g}})} \tag{8}$$

where λ is the spin-orbit coupling constant and ΔE are the excitation energies. Using the literature values of $\Delta E(^3\mathrm{B}_{1\mathrm{g}} \rightarrow {}^3\mathrm{E}_{\mathrm{g}}) = 7480$ cm^{-1}, $\Delta E(^3\mathrm{B}_{1\mathrm{g}} \rightarrow {}^3\mathrm{B}_{2\mathrm{g}}) = 12130$ cm^{-1}, and $g_{\mathrm{iso}} = 2.18$ [3], we obtained $g_{\perp} = 2.21$ and $g_{\parallel} = 2.13$. The geometric parameters R were taken from the crystal structure, whereas Ω were approximated by zero for all the nuclei in the imidazole ligand, on the assumption that S–Ni–S was the symmetric axis. We finally obtained an expression of the isotropic NMR shift as

$$\delta_{\mathrm{iso}}/\mathrm{ppm} = \left[\frac{22.9 \cdot A/\mathrm{MHz}}{\gamma_{\mathrm{nuc}}/\gamma_{^1\mathrm{H}}} + \frac{47}{(R/\text{Å})^3}\right] x + \delta_{\mathrm{dia}}/\mathrm{ppm} \tag{9}$$

where x is defined as

$$x = \frac{1000}{T/\mathrm{K} - 15.3}, \tag{10}$$

and δ_{dia} is assumed to be independent of temperature.

Temperature dependence of the isotropic shifts of ^{1}H-,^{2}H- and ^{13}C-MAS-NMR of **3** were fitted by Eq. 9 as shown in Fig. 4. The experimental values of A are listed in Table 2 where the hfccs of deuteron were converted to those of proton by multiplying by the gyromagnetic ratio $\gamma_{^1\mathrm{H}}/\gamma_{^2\mathrm{H}}$. We observed that

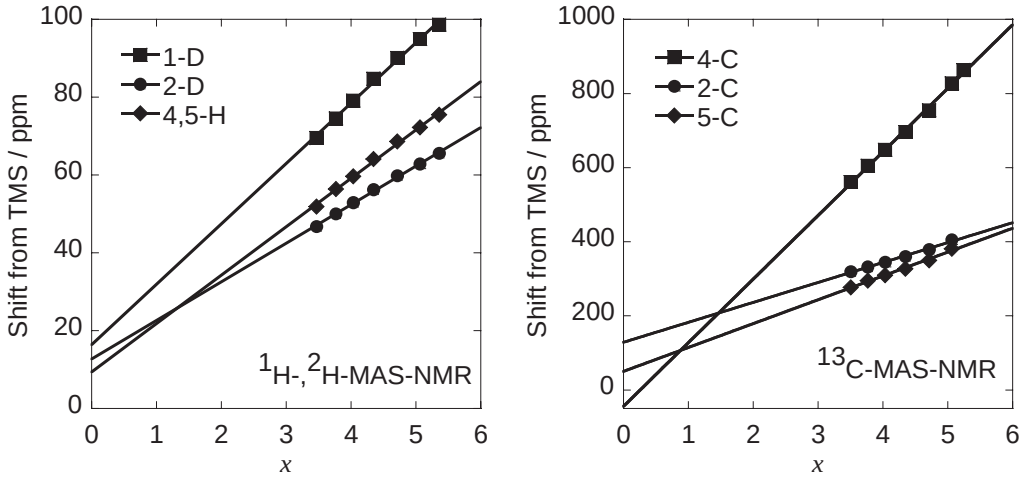

Fig. 4. Temperature dependence of the isotropic shifts of ^{1}H-,^{2}H- and ^{13}C-MAS-NMR of **3**. The variable x is defined to be $x = 1000/(T/\mathrm{K} - 15.3)$ and is proportional to the magnetic susceptibility. The solid lines are the result of fitting to Eq. 9.

A of H and C are all positive values. The sign of A^{calc} obtained from DFT calculation were also positive and the $(A^{\mathrm{calc}} - A^{\mathrm{exp}})/A^{\mathrm{exp}}$ were within ± 20 % for carbon. This agreement between the experimental and theoretical hfcc encouraged us to utilize the calculated atomic spin density ρ^{calc} for discussing the spin density distribution of the imidazole ligand.

3.3 Spin density distribution of the imidazole ligand and possible interchain pathway

The positive signs of A of H and C can be explained by σ spin delocalization mechanism.[22] An octahedral Ni^{2+} $(S = 1)$ complex has a $(\mathrm{t_{2g}})^6(\mathrm{e_g})^2$ configuration and $\mathrm{e_g}$ orbitals are the SOMO of this complex. One of the $\mathrm{e_g}$ orbitals is composed of $\mathrm{d}_{x^2-y^2}$ orbital of the nickel ion and σ orbitals of the ligand

$$\mathrm{e_g} = c_{\mathrm{d}}\mathrm{d}_{x^2-y^2} + \sum_{k=1}^{4} c_k\sigma_k \tag{11}$$

Table 2

Hyperfine coupling constant A / MHz and atomic spin density ρ of the imidazole ligand in $Ni(NCS)_2(Him)_2$ crystal.

position	A^{exp}	A^{calc}	ρ^{calc}
1-^{14}N	—	+0.81	+0.001
2-^{13}C	+0.57	+0.46	−0.007
3-^{14}N	—	+18.5	+0.057
4-^{13}C	+0.69	+0.85	−0.003
5-^{13}C	+1.88	+1.88	+0.003
1-^{1}H	+0.66	+0.45	
2-^{1}H	+0.37	+0.52	
4-^{1}H	+0.48	+0.63	
5-^{1}H	+0.53	+0.36	

where c_{d} and c_k are appropriate coefficients. In the case of nickel-imidazole complexes, one of the σ orbitals is the n-orbital or a molecular orbital occupied by lone electron-pair, which is mainly composed of an atomic orbital (AO) of 3-nitrogen. The coefficients of Eq. 11 is related to the spin delocalization from nickel into 3-nitrogen and the degree of the delocalization was $|c_{\mathrm{Him}}|^2 \simeq 0.06$ for $Ni(NCS)_2(Him)_2$ as is seen in Table 2. The electron spin is delocalized over the whole imidazole ligand because the n-orbital is not only composed of the AO of 3-nitrogen, but also of s-orbitals of hydrogen atoms and sp^2 orbitals of carbon atoms of the ligand. Though the contributions from these other AOs are small compared to that of the 3-nitrogen, the result that *all* of the observed

A of H and C are positive values indicates that the σ spin delocalization is the dominant mechanism.

The other possible mechanism that induces spin density distribution is spin polarization mechanism, originally introduced by McConnell and Chesnut to explain negative spin densities in aromatic radicals. It states that in molecular orbital theory the most likely spot to find a negative spin density is on a carbon atom which has zero spin density in the ground state configuration.[23] Subsequently, it was extended to deal with non-aromatic radicals such as nitroxide or nitronyl nitroxide. It is sometimes referred to as alternation rule because the sign of the spin density alternates through successive bonds.[24] In the imidazole ligand of $Ni(NCS)_2(Him)_2$, the spin source that induces π spin polarization is the p_z orbital of 3-nitrogen of which electron spin is induced by n-π spin polarization. The alternation rule predicts negative spin densities on 2- and 4-carbon atoms and positive spin densities on 1-nitrogen and 5-carbon from this spin source. The calculated atomic spin densities ρ^{calc} listed in Table 2 are explained by this alternation rule but the experimental and theoretical hfccs are not. We thus concluded that the spin polarization dominates atomic spin densities of the π-electron systems in the imidazole ligand but the σ-electron systems is dominated by σ spin delocalization. The effect of the spin polarization on the σ-electron systems can be seen from the difference between hfcc of 5-carbon and those of 2,4-carbon in magnitude. Larger hfcc of 5-carbon indicates that the σ spin delocalization and the π spin polarization work cooperatively at this site but counterwork on 2,4-carbon atoms. It should be emphasized that the effect of the π spin polarization is negligible on hydrogen atoms, judging from the value of hfcc, and this positive spin densities of s-orbitals of the hydrogen atoms are brought by the σ spin

delocalization. In other words, SOMO of this complex extends into the whole imidazole ligand.

The observed spin density distribution of the imidazole ligand in $Ni(NCS)_2(Him)_2$ qualitatively agreed with those of $[Ni(Him)_6]^{2+}$[22] and $Cu(Him)_2Cl_2$[25]. The nature of σ delocalization is independent of environment. Here we briefly discuss the intermolecular magnetic interaction via the imidazole ligand. On the basis of above discussion, the $d_{x^2-y^2}$-based SOMO of $Ni(NCS)_2(Him)_2(SCN)_2$ unit is extended to 1-hydrogen that forms hydrogen bond with a sulfur atom of an adjacent chain as shown in Fig. 5(a). A p-orbital of this sulfur atom has MO coefficient of the other SOMO mainly composed of d_{z^2} of the nickel atom. Therefore, orthogonal SOMO-SOMO interaction occurs at N–H $\cdots$ S hydrogen bond. This causes a ferromagnetic interaction between the chains. In the case of $Cu(Him)_2Cl_2$, the $d_{x^2-y^2}$-based SOMO extended to 1-hydrogen has finite overlap integral between the SOMO of the adjacent Cu(II) complex (Fig. 5(b)). Thus antiferromagnetic interaction occurs at N–H $\cdots$ Cl hydrogen bond. Imidazole ligand acts as either ferromagnetic or antiferromagnetic exchange coupler, depending on the crystal packing.

Acknowledgements

This research was supported by grant-in-aid for Scientific Research (Nos. 14740371 and 15087201) from the Ministry of Education, Culture, Sports, Science and Technology of Japan.

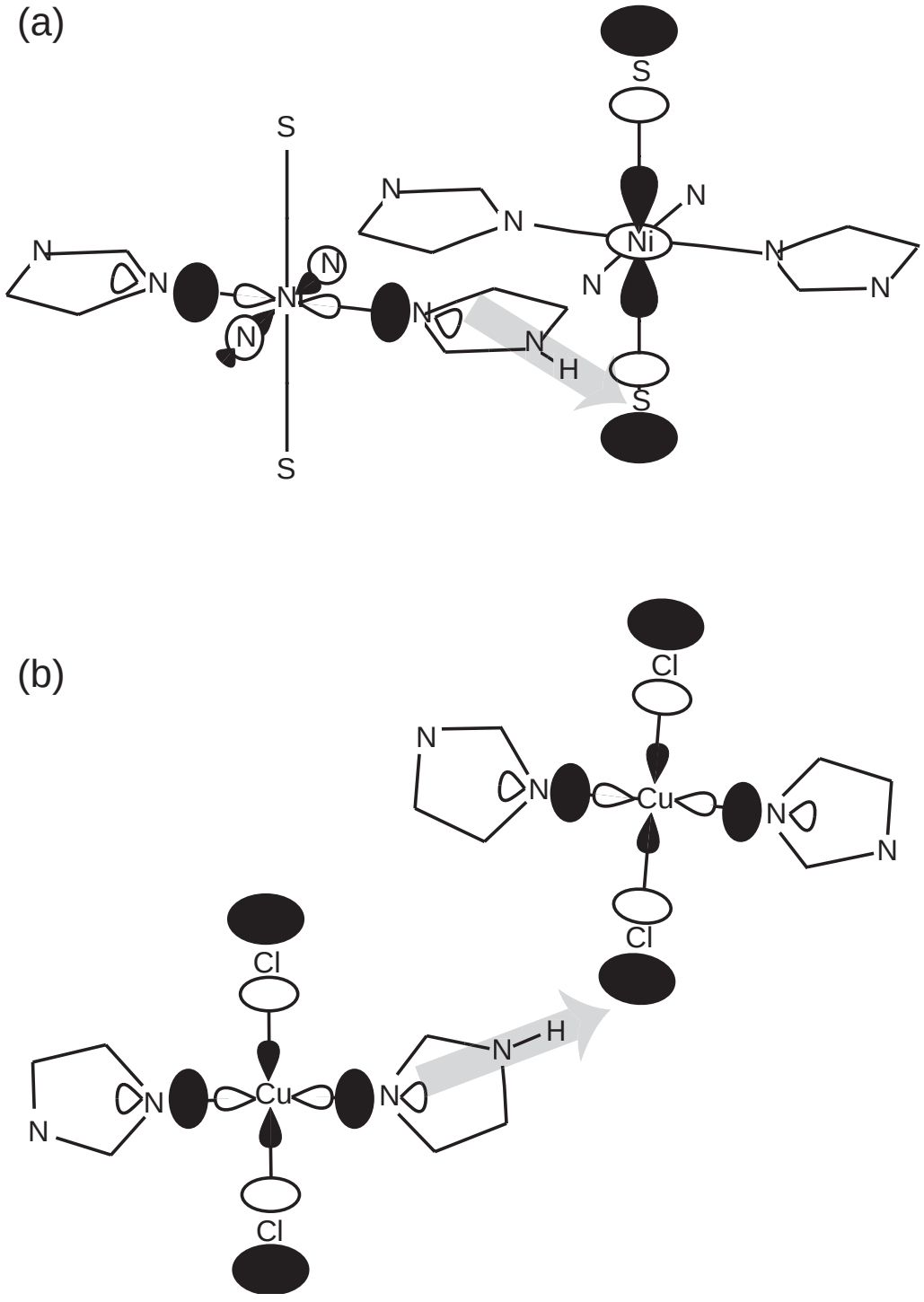

Fig. 5. Interchain SOMO-SOMO interactions via imidazole ligands in (a) $Ni(NCS)_2(Him)_2$ and (b) $Cu(Him)_2Cl_2$. Black and white represent opposite signs of the SOMO. The gray arrows indicate the delocalized SOMOs which extend onto the chain-bridging imidazole ligands. (a) Ferromagnetic interaction between the $d_{x^2-y^2}$-based and the d_{z^2}-based SOMOs. N–H bond is directed toward the *node* of the p-orbital of the sulfur. N$\cdots$S distance is 3.38 Å and N$\cdots$S–Ni angle is 92.7°[3]. (b)Antiferromagnetic interaction between the $d_{x^2-y^2}$-based SOMOs. N–H bond is directed toward the outer *lobe* of the p-orbital of the chlorine. N$\cdots$Cl distance is 3.16 Å and N$\cdots$Cl–Cu angle is 135.2°[7].

References

[1] S.J. Blundell, F.L. Pratt, J. Phys.: Condens. Matter 16 (2004) R771.

[2] J.V. Yakhmi, Macromol. Symp. 212 (2004) 141.

[3] B. Żurowska, J. Mroziński, M. Julve, F. Lloret, A Maslejova, W. Sawka-Dobrowolska, Inorg. Chem. 41 (2002) 1771.

[4] J. Cano, P.S. Alemany, M. Verdaquer, E. Ruiz, Chem. Eur. J. 4 (1998) 476.

[5] F. Fabrizi de Biani, E. Ruiz, J. Cano, J.J. Novoa, S. Alvarez, Inorg. Chem. 39 (2000) 4271.

[6] B. Gillon, Spin Distributions in molecular systems with interactint transition metal ions. In Magnetism: Molecules to Materials, J.S. Miller, M. Drillon Eds. (WILEY-VCH, Weinheim, 2001) 357.

[7] B.K.S Lundberg, Acta Chem. Scand. 26 (1972) 3977.

[8] W.E. Estes, W.E. Hatfield, J.A.C. van Ooijen, J. Reedijk, J.C.S. Dalton (1980) 2125.

[9] F.H. Köhler, Probing spin densities by use of NMR spectroscopy. In Magnetism: Molecules to Materials, J.S. Miller, M. Drillon Eds. (WILEY-VCH, Weinheim, 2001) 379.

[10] R.J. Gillespie, A. Grimison, J.H. Ridd, R.F.M. White, J. Chem. Soc. (1958) 3228.

[11] A. Bielecki, D.P. Burum, J. Magn. Reson. A116 (1995) 215.

[12] The difference $T - T_{\mathrm{b}}$ originates from frictional heating, heat from the driving gas of room temperature, and uncalibrated T_{b}.

[13] M.J. Frisch, G.W. Trucks, H.B. Schlegel, G.E. Scuseria, M.A. Robb, J.R. Cheeseman, V.G. Zakrzewski, J.A. Montgomery, Jr., R.E. Stratmann, J.C. Burant, S. Dapprich, J.M. Millam, A.D. Daniels, K.N. Kudin, M.C. Strain, O. Farkas, J. Tomasi, V. Barone, M. Cossi, R. Cammi, B. Mennucci, C. Pomelli, C. Adamo, S. Clifford, J. Ochterski, G.A. Petersson, P.Y. Ayala, Q. Cui, K. Morokuma, P. Salvador, J.J. Dannenberg, D.K. Malick, A.D. Rabuck, K. Raghavachari, J.B. Foresman, J. Cioslowski, J.V. Ortiz, A.G. Baboul, B.B. Stefanov, G. Liu, A. Liashenko, P. Piskorz, I. Komaromi, R. Gomperts, R.L. Martin, D.J. Fox, T. Keith, M.A. Al-Laham, C.Y. Peng, A. Nanayakkara, M. Challacombe, P.M.W. Gill, B. Johnson, W. Chen, M.W. Wong, J.L. Andres, C. Gonzalez, M. Head-Gordon, E.S. Replogle, and J.A. Pople, GAUSSIAN 98, Revision A.11.1, Gaussian, Inc., Pittsburgh PA, 2001.

[14] A.J.H. Wachters, J. Chem. Phys. 52 (1970) 1033.

[15] P.J. Hay, J. Chem. Phys. 66 (1977) 4377.

[16] H. Lee, T. Polenova, R.H. Beer, A.E. McDermott, J. Am. Chem. Soc 121 (1999) 6884.

[17] J. Herzfeld, A.E. Berger, J. Chem. Phys. 73 (1980) 6021.

[18] WIN-FIT, ver. 950425, Bruker-Franzen Analytik.

[19] C.P. Slichter, Principles of Magnetic Resonance, 3rd edition, chapter 4 (Springer-Verlag, Berlin, 1990).

[20] T. Sandreczki, D. Ondercin, R.W. Kreilick, J. Magn. Reson. 34 (1979) 171.

[21] R.J. Kurland, B.R McGarvey, J. Magn. Reson. 2 (1970) 286.

[22] M. Wicholas, R. Mustacich, B. Johnson, T. Smedley, J. May, J. Am. Chem. Soc. 97 (1975) 2113.

[23] H.M. McConnell, D.B. Chesnut, J. Chem. Phys. 27 (1957) 984.

[24] G. Maruta, S. Takeda, R. Imachi, T. Ishida, T. Nogami, K. Yamaguchi, J. Am. Chem. Soc. 121 (1999) 424.

[25] G. Maruta, S. Takeda, preliminary results of ^{2}H-, ^{13}C-MAS-NMR experiment: $A_{^{13}\mathrm{C}} = 0.6 \sim 4.6$ MHz, $A_{^{1}\mathrm{H}} = 0.81 \sim 2.20$ MHz.